Protein phosphatase 2C, AP2C1 interacts with and negatively regulates the function of CIPK9 under potassium deficient conditions in *Arabidopsis*

Amarjeet Singh[1, #], Akhilesh K. Yadav[1], Kanwaljeet Kaur[1], Sibaji K. Sanyal[1], Saroj K. Jha[1], Joel L. Fernandes[1], Pankhuri Sharma[1], Indu Tokas[1], Amita Pandey[1], Sheng Luan[2], Girdhar K. Pandey[1,*]

[1]Department of Plant Molecular Biology, University of Delhi South Campus, New Delhi, India
[2]Department of Plant and Microbial Biology, University of California Berkeley, Berkeley, California, USA

[*]Corresponding author: **Girdhar K. Pandey,**
Tel: +91-11-24116615, Fax: +91-11-24111208
Email: gkpandey@south.du.ac.in

Present address- National Institute of Plant Genome Research, New Delhi, India

Email Id of co-authors: singh.amarjeet07@gmail.com; akhilesh_du@yahoo.co.in; kanwaljeet008@gmail.com; sanyalsibaji@gmail.com; saroj.pmb@gmail.com; joel.lars.fernandes@gmail.com; pankhuri.pmb@gmail.com; indutokas16@yahoo.co.in; amitap04@gmail.com; sluan@berkeley.edu

Running title: AP2C1 regulate CIPK9 function in K^+ deficiency

Highlight

AP2C1 interacts with CIPK9 *in vitro* and *in planta*. AP2C1 dephosphorylate CIPK9, thereby negatively regulates its function in low-K^+ conditions. The kinase-phosphatase pair provide a crucial regulatory mechanism of low-K^+ responses in plants.

Abstract

Potassium (K^+) is a major macronutrient required for plant growth. In response to low- K^+ condition, an adaptive mechanism entails activation of the Ca^{2+} signaling network consisting of calcineurin B-like proteins (CBLs) and their interacting kinases (CIPKs) in plants. The CBL-interacting protein kinase 9 (CIPK9) is previously implicated in low-K^+ responses in *Arabidopsis thaliana*. Here, we report a protein phosphatase 2C (PP2C), AP2C1, as an interactor of CIPK9. Fluorescence resonance energy transfer (FRET), bimolecular fluorescence complementation (BiFC) and co-localization analyses revealed that CIPK9 and AP2C1 interact in the cytoplasm. AP2C1 dephosphorylates the auto-phosphorylated form of CIPK9 *in vitro*, presenting a regulatory mechanism for CIPK9 function. Furthermore, genetic and molecular analysis revealed that *ap2c1* null mutants (*ap2c1-1* and *ap2c1-2*) are tolerant to low-K^+ conditions, retained higher K^+ content and showed higher expression of K^+ deficiency related genes contrary to *cipk9* mutants (*cipk9-1* and *cipk9-2*). In contrast, transgenic plants overexpressing AP2C1 were sensitive to low-K^+ conditions. Thus, this study shows that AP2C1 and CIPK9 interact to regulate K^+-deficiency responses in *Arabidopsis*. CIPK9 functions as positive regulator whereas, AP2C1 acts as a negative regulator of *Arabidopsis* root growth and seedling development under low-K^+ conditions.

Keywords: Arabidopsis, Calcium signaling, CBL-interacting protein kinase, Dephosphorylation, Phosphorylation, Potassium deficiency, Protein phosphatase 2C, Regulation.

Introduction

Potassium (K^+) is the most abundant cation and an essential macronutrient in living plant cell. It constitutes almost 10% of the plant's dry weight and is vital in many physiological processes in plant cells including, electrical neutralization, enzyme activation, stomata movement, membrane potential maintenance, and osmotic regulation (Han *et al*., 2016). Moreover, K^+ participate to accentuate photosynthesis, starch synthesis, and transport of assimilates, thereby ultimately determines crop yield and productivity (Pettigrew, 2008; Zörb *et al*., 2014). In the cytoplasm, K^+ concentration remains stable at approximately 100 mM (Walker *et al*., 1996) however; its concentration in the soil at the root surface is generally as low as 1mM (Schroeder *et al*., 1994; Maathuis, 2009).

K^+ deficiency adversely affects plant growth and development due to its requirement in several vital cellular processes (Wang and Wu, 2013). In order to counteract and adapt to K^+ deficient environment, plants have devised complex signaling and physiological regulatory systems (Wang and Wu, 2013). One of the major mechanisms is maintenance of cellular K^+ homeostasis, which

involves uptake and transport of K^+ across different membranes (Amtmann and Armengaud, 2007). Extensive molecular analysis of K^+ transport system has suggested two main mechanisms of K^+ acquisition; high affinity and low affinity uptake through roots. High-affinity K^+ uptake is carried out by transporters at low external K^+ concentrations (as low as 10μM), whereas low affinity uptake and transport is mediated by K^+ channels at relatively higher external K^+ concentrations (above 100μM) (Pyo *et al*., 2010; Rubio *et al*., 2008; Shin, 2014).

Under low-K^+ condition, a specific Ca^{2+} signal is generated through an unknown mechanism (Behera *et al*., 2017) and transduced downstream by a CBL-CIPK module in *Arabidopsis* (Singh *et al*., 2016). Ca^{2+} signal is generally perceived by the Ca^{2+} sensors and their interactors/targets. The CBL proteins have been recognised as crucial Ca^{2+} sensors in plant cell (Pandey, 2008; Luan, 2009). CBLs interact with CBL-interacting protein kinases (CIPKs), a family of plant serine/threonine kinases (Pandey, 2008; Luan, 2009; Pandey *et al*., 2014). A total of 10 CBLs and 26 CIPKs isoforms have been identified in *Arabidopsis* genome. Different CBL-CIPK isoforms constitute diverse interacting network to regulate Ca^{2+} signaling pathways (Luan, 2009; Weinl and Kudla, 2009; Pandey *et al*., 2014). Under K^+ deficient conditions, CBL1/CBL9-CIPK23 complex localizes to plasma membrane of root hair cells, where CIPK23 phosphorylates a voltage-dependent potassium channel AKT1 (*Arabidopsis* K^+ transporter 1) to enhance K^+ uptake (Li *et al*., 2006; Xu *et al*., 2006). In a reverse genetic screen, CIPK9 was identified as an important regulator of K^+ deficiency response in *Arabidopsis* (Pandey *et al*., 2007). Loss-of-function of CIPK9 leads to enhance sensitivity on low- K^+ media in terms of plant growth, suggested that CIPK9 functions as a positive regulator of low-K^+ tolerance (Pandey *et al*., 2007). Besides CIPKs, CDPKs and SnRK2s have been found to regulate K^+ channels, which are involved in stomata movement during drought stress. For example; *Arabidopsis* AtCPK13 at guard cell phosphorylate inward rectifying K^+ channels AtKAT1 and AtKAT2. Similarly, AtSnRK2.6 (AtOST1) phosphorylate AtKAT1 leading to its inactivation, thereby, promoting stomata closure (Simeunovic *et al*., 2016). Furthermore, AtCPK3, 4, 5, 11 and 29 phosphorylate the two pores K^+ channel (AtTPK1), which is responsible for K^+ efflux from the vacuole in *Arabidopsis* (Latz *et al*., 2013; Simeunovic *et al*., 2016).

Protein phosphatases 2C (PP2Cs) are known as counteracting molecule to kinases in general, and also involves in K^+ deficiency triggered signaling (Chérel *et al*., 2002; Lee *et al*., 2007; Singh *et al*., 2016). While, CBL1/CBL9-CIPK23 complex function to activate AKT1 through phosphorylation, a PP2C, AIP1 deactivate AKT1 by dephosphorylation (Li *et al*., 2006; Lee *et al*., 2007). This CBL1/CBL9-CIPK23-AKT1-AIP1 module is the primary signaling cascade known to regulate K^+ uptake in plants till date (Wang and Wu, 2017). AtPP2CA interacts with *Arabidopsis* K^+

transporter AKT2, which is a weak inward rectifier channel. Co-expression of AtPP2CA and AKT2 in COS cells and *Xenopus* oocyte resulted in inhibition of AKT2 inward rectification current. Inhibition of AKT2 mediated current was due to dephosphorylation of AKT2 by AtPP2CA (Chérel *et al*., 2002) Additionally, it was found that the activity of AKT2 channel and its translocation from endoplasmic reticulum to plasma membrane was regulated by CBL4-CIPK6 complex through their interaction, but independent of phosphorylation activity (Held *et al*., 2011). Till date, no kinase have been identified at the molecular level, which could phosphorylate AKT2 (Wang and Wu, 2013). Therefore, phosphorylation and dephosphorylation of K^+ channels is an important regulatory mechanism of K^+ uptake and homeostasis under low-K^+ conditions.

In this study, we have identified a protein phosphatase 2C, AP2C1 as an interactor of CIPK9. Physical interaction of AP2C1 and CIPK9 was confirmed by yeast two-hybrid and protein pull-down assay. *In planta* interaction of two proteins was established by FRET, BiFC and co-localization assays. Biochemical activity analysis showed that AP2C1 dephosphorylate auto-phosphorylated CIPK9, which could be the possible regulatory mechanism of CIPK9 function *in vivo*. Genetic and molecular analysis of AP2C1 and CIPK9 null mutants and AP2C1 overexpressing transgenic plants suggested the functional involvement of CIPK9 and AP2C1 in the same signaling pathway to regulate the K^+ deficiency response in *Arabidopsis*.

Material and Methods

Constructs preparation and yeast two-hybrid analysis

Complete amplified open reading frame (ORF) of *AP2C1* and *CIPK9* were inserted at *BamH*I and *Sal*I restriction sites of both activation-domain (pGAD.GH) and DNA binding domain (pGBT9.BS) vectors (Clontech). Similarly, different *AP2C1* deletion fragments (K1, K2, K3, KIM and PP2Cc) and other fragments were cloned in *BamH*I and *Sal*I restriction sites of both pGAD.GH and pGBT9 vectors. All the clones were confirmed by sequencing. Primers are listed in Supplemental Table S1. To examine the physical interaction between the AP2C1 and CIPK9, AD-AP2C1 and BD-CIPK9 (and also vector swap) plasmids were co-transformed into yeast strain AH109 and yeast two-hybrid experiments were performed according to Pandey *et al*., 2015. Similar analysis was also performed for AP2C1 with all 26 members (including CIPK9) of *Arabidopsis* CIPK family, and for CIPK9 with PP2Cs, which are homologs of AP2C1 and previously implicated in K^+ deficiency response (Lee *et al*., 2007; Lan *et al*., 2011).

Protein expression and purification

To express protein in *E. coli*, complete ORF lacking stop codon of *AP2C1* and *CIPK9* were amplified and cloned in fusion with GST and 6X His tags of pGEX4T-1(GE HealthCare, USA) and pET28a (Novagen) vectors, respectively, at *BamH*I and *Sal*I restriction sites. All the clones were confirmed by sequencing and the primers are listed in Table S1. Protein expression and purification were carried out according to Sanyal *et al*., 2017.

Site directed mutagenesis of AP2C1 (G178D)

The substitution of Gly^{178} (G) to Asp^{178} (D) in the AP2C1 ORF was carried out according to the Quick Change Site-directed Mutagenesis® instruction manual (Stratagene) using following primer pair AP2C1G/D F: TTCGGAGTCTATGATGGTCATGACGGAGTTAAAGC GGCTGAGTTT, AP2C1G/D R: AAACTCAGCCGCTTTAACTCCGTCATGACCATCA TAGACTCCGAA. Mutagenesis reactions were conducted on AP2C1/pDONOR (ABRC, Ohio) plasmid DNA. A 50µl PCR reaction was set up using 50ng of template plasmid, 200µM of dNTPs, 125ng of primers and 1 unit of PrimeSTAR™ DNA polymerase (Takara, Japan). The PCR condition for the reaction was: 98°C for 4 minutes, followed by 18 cycles of 98°C for 30seconds, 68°C for 1 minute, 72 °C for 6 minutes followed by final extension at 72 °C for 10 minutes. The construct was verified for the mutagenesis by sequencing. The mutated AP2C1 (G178D) sequence was amplified and sub-cloned into pGEX4T-1 for protein expression.

***In vitro* GST-pull down assay**

Recombinant proteins with GST tag were purified using Glutathione-sepharose 4B according to manufacture instructions (GE-healthcare, UK). The 6X-His tag expressing proteins were induced using 0.1mM isopropyl-1-thio-b-D-galactopyranoside (IPTG) at 30°C for 6 hours. The expressed soluble protein was extracted in 1X phosphate buffer saline (pH-7.5) with lysozyme and sonication. The purified protein was quantified by loading onto 10% SDS-PAGE gel and staining with coomassie brilliant blue. The Glutathione-sepharose 4B bound GST and GST-fused proteins (approximately 1µg) were incubated with bacterial soluble lysate expressing 6X-His fusion proteins for 4 hours at 4°C. The beads were washed six times with phosphatebuffer saline at 4°C. Protein

complex bound to the beads were boiled in 2X SDS sample buffer for 5 minutes and separated by 10% SDS-PAGE. Proteins were transferred to nitrocellulose membrane. Immunoblotting was performed using anti-His antibody (1:5000 dilution) and loading- controls were shown by anti-GST (1:500 dilution) antibody.

In vitro phosphatase activity assay

Purified GST-CIPK9, GST-AP2C1 and GST-AP2C1 (G178D) proteins were quantified with known concentration of purified bovine serum albumin (BSA). *In vitro* assay was performed in reaction buffer (20mM Tris pH 7.2, 2.5mM $MnCl_2$, 0.5mM $CaCl_2$, 1mM DTT, 10µM ATP and 5µCi $^{32}\gamma P$) with different combination of affinity purified GST-CIPK9 (1µg) and GST-AP2C1(500ng) proteins in 30µl reaction. The reaction was performed at 30^{o}C for 30 min. and terminated by 1x SDS-PAGE loading buffer. These reactions were loaded onto 10% SDS-PAGE, after resolution gel was dried and signals were developed by exposing the dried gel to X-ray film by autoradiography methodology. To determine the dose dependent phosphatase activity of AP2C1, different concentration of GST-AP2C1 and GST-AP2C1 (G178D) (10ng to 250 ng) were used with constant amount of GST-CIPK9 (500ng).

FRET analysis

The complete ORFs lacking stop codon of *CIPK9* and *AP2C1* were amplified from cDNA, cloned in pENTR-D/TOPO (Invitrogen) and subsequently mobilized to gateway compatible binary vector pSITE 3CA (YFP Tag) and pSITE 1CA (CFP tag), respectively (Chakrabarty *et al*., 2007). Primers are listed in Supplemental Table S1. *Nicotiana benthamiana* plants were transiently transformed with *Agrobacterium tumefaciens* GV3101::pMP90 carrying AP2C1-CFP, KIM-CFP and K2-CFP constructs in combination with YFP-CIPK9 according to Singh *et al*., 2013. Transformed cells were analysed using confocal microscope (TCS SP5; Leica). The cells showing expression of both CFP and YFP were selected for FRET analysis by acceptor bleaching protocol. FRET efficiency was recorded in more than three cells at a time. CFP was excited by argon laser at 458 nm and emissions were collected between 465 nm and 505 nm, whereas YFP was excited at 512 nm and emissions were collected between 525 nm and 600 nm. Combination of empty vector of pSITE3CA and pSITE1CA was co-transformed as a negative control.

BiFC and Co-localization

Amplified ORF of *AP2C1* was inserted at *Bam*HI and *Sal*I restriction sites of binary vector, pGPTVII.GFP.Kan. The CDS of *CIPK9* was cloned in Gateway® entry vector pENTR-D/TOPO (Invitrogen) and subsequently mobilized to gateway compatible binary vector pSITE 4CA . Primers are listed in Supplemental Table S1. These constructs were used to transform *N. benthamiana* cells as describe earlier. For co-localization, overnight grown cultures of *Agrobacterium* carrying AP2C1-GFP and RFP-CIPK9 were mixed and infiltrated into *N. benthamiana* cells. For BiFC, ORFs of AP2C1 and CIPK9 were mobilized using Gateway technology from pENTR-D/TOPO vector to pSPYCE-35S^{GW} and pSPYNE-35S^{GW}, respectively. *Agrobacterium* GV3101::pMP90 carrying the BiFC constructs were co-infiltrated in *N. benthamiana* cells.

Confocal Microscopy

Transiently transformed *N. benthamiana* epidermal peel cells were analyzed in confocal microscope to detect the fluorescence. Confocal microscopy was performed according to Singh *et al*., 2014.

Plant materials and growth conditions

Arabidopsis thaliana ecotype Columbia-0 was used for generation of overexpression transgenic plants. *Arabidopsis* seeds were surface sterilized and grown according to Singh *et al*., (2015).

Isolation of T-DNA insertion mutants

The homozygous mutant allele *ap2c1-1* (SALK_065126) was kindly provided by Dr. Irute Meskiene (Max F. Perutz Laboratories, University of Vienna, Austria). The *ap2c1-2* mutant allele was isolated from T-DNA insertion collection of Arabidopsis Biological Resource Centre (ABRC, Ohio, USA)-SALK (http://signal. salk.edu/; SALK_104445). T-DNA insertion and its genomic position were confirmed by PCR using a T-DNA left border and a gene specific primer. After the selfing of heterozygous plants, homozygous *ap2c1-2* mutant allele was identified and disruption of native AP2C1 gene was confirmed by genomic DNA PCR. Disruption of the gene expression in both *ap2c1-1* and *ap2c1-2* alleles was confirmed by semi-quantitative RT-PCR analysis. Homozygous CIPK9 mutant alleles, *cipk9-1* and *cipk9-2* used in this study were already confirmed by Pandey *et al*., (2007).

Overexpression transgenic plant generation

To generate *Arabidopsis* overexpression constructs, complete ORF of *AP2C1* was PCR amplified and cloned at *BamH*I and *Sal*I restriction sites of modified pCAMBIA1300 vector under the control of CaMV 35S promoter. Primers used are listed in Supplemental Table S1. Overexpression transgenic plants were generated according to Singh *et al*., 2015. Transgenic plants confirmed for AP2C1 overexpression by qPCR (according to Singh *et al*., 2012) and used for further analysis.

Preparation of modified MS growth media with variable K^+ levels

To perform phenotype analysis on K^+ deficient conditions, modified MS medium containing different concentrations of KCl was prepared in double distilled deionized water. This modified media contains K^+ free 1/20 strength of MS major salts and 1X MS minor salts. K^+ free medium was prepared by replacing MS salts with the following (1×MS): 1650 mg/l NH_4NO_3, 440 mg/l $CaCl_2 \cdot 2H_2O$, 370 mg/l $MgSO_4 \cdot 7H_2O$, 165 mg/l $(NH_4)_2HPO_4$, 27.8 mg/l $FeSO_4 \cdot 7\ H_2O$, 37.3 mg/l di-sodium EDTA, 0.7495 mg/l NaI, 6.3 mg/l H_3BO_3, 16.9 mg/l $MnSO_4 \cdot H_2O$, 8.6 mg/l $ZnSO_4 \cdot 7H_2O$, 0.25 mg/l $Na_2Mo_4 \cdot 2H_2O$, 0.016 mg/l $CuSO_4 \cdot 5H_2O$, and 0.0267 mg/l $CoSO_4 \cdot 6H_2O$. For solidification of the media 1% agarose (Sigma-Aldrich, USA) was used. Varying level of K^+ were achieved by adding KCl to the K^+ free media.

Phenotype and root elongation assays

Arabidopsis seeds each from the WT (Col-0), *cipk9* mutant alleles (*cipk9-1* and *cipk9-2*), *ap2c1* mutant alleles (*ap2c1-1* and *ap2c1-2*) and *AP2C1 OX* transgenic lines seeds were surface sterilized as described earlier. Approximately 30 seeds were planted on modified MS-agarose medium with different concentrations of K^+ and incubated at 4 °C for 4 days for stratification and then transferred to 22°C growth chamber under long-day (16 h light, 8 h dark) conditions. Phenotype and root growth assays were carried out by placing the plates vertically on a rack. Relative root growth and relative fresh weight of seedlings were determined as the ratio of root growth or fresh weight of seedlings for respective mutant allele or overexpression line to wild type at a particular K^+ concentration. Experiments were repeated three times and quantitative data is presented as mean ± SD from three observations.

K^+ content estimation by atomic absorption spectroscopy

Arabidopsis seeds were surface sterilized and plated on Whatmann filter paper 1. The plates were supplemented with 1/20 strength (major salts) MS media. The seeds were allowed to grow under

long-day conditions with 200 µE m^{-2} s^{-1} light intensity, 75% humidity, and 22 °C. After 10 days of growth, seedlings were washed about 6-8 times with double distilled Milli Q water to remove traces of K^+. The seedlings were then supplemented with 10µM and 10mM KCl solution to prepare K^+ deficient and control samples, respectively. After 14 days, the K^+ deficient and control seedlings were harvested and oven dried for 48 hrs at 50° C. 10mg dried tissue was weighed in separate 15 mL test tubes, digested with 1mL conc. HNO_3 and concentrated to about 100µL at 65°C in an oven. The digested concentrate was re-dissolved to 10mL using double distilled Milli Q water. The ion content in the samples were then analysed using the Analyst 400 Atomic absorption spectroscope (Perkin Elmer, USA). A standard curve was plotted using known standard concentrations of K^+. The experiment was performed at least three times using three technical and biological replicates.

K^+ deficiency treatment and expression analysis by qPCR

The *Arabidopsis* seeds for different genotypes were surface sterilized and grown similar to K^+ content estimation. After 10 days of growth, plants were treated with K^+ sufficient (10mM K^+) and K^+ deficient (10 µM K^+) media for five days. Treated and control seedlings were collected in replicates and immediately frozen in liquid N_2. Total RNA isolation and cDNA preparation was carried out according to Singh *et al*., (2015) and qPCR expression analysis was performed according to Singh *et al*., (2012).

Statistical analysis

All the expression, phenotypic, and quantitative experiments have been replicated thrice and the data has been presented as mean ± S.D (standard deviation). Two tailed student's t-test was performed to determine the statistical significance among the samples. A p-values <0.05 was considered statistically significance.

Results

AP2C1 physically interacts with CIPK9

CIPK9 was identified as a positive regulator of K^+ deficiency signalling in *Arabidopsis* (Pandey *et al*., 2007). In order to identify the upstream and downstream components of CIPK9 mediated

signaling, a yeast two-hybrid library screening was performed. AP2C1 was identified as one of the putative interactors of CIPK9 in the library screening. To confirm the interaction, target based yeast two-hybrid assays were performed. Yeast cells co-transformed with AP2C1 and CIPK9 proliferated on the selection media SC-Leu,-Trp,-His (SC-LWH) and SC-LWH media containing 0.5 mM and 3.0 mM of 3-Amino-1,2,3-triazole (3-AT). Similar, growth pattern was observed when vectors were swapped (Fig. 1A). No growth was seen for negative controls: AP2C1.BD/AD, CIPK9.BD/AD and AD/BD on the same medium. An *in vitro* GST pull down assay was also performed, where *E. coli* expressing GST-CIPK9 and His-AP2C1 were used for analysis. Probing with anti-6XHis antibody showed a strong band in western blot analysis, corresponding to the size of AP2C1 when both His-AP2C1 and GST-CIPK9 were present in the reaction (Fig. 1B). The growth pattern of yeast and GST protein pull-down assays confirm the physical interaction between AP2C1 and CIPK9 proteins. Moreover, interaction analysis of AP2C1 with all the *Arabidopsis* CIPK members (CIPK1-26), and that of CIPK9 with other PP2Cs e.g. AIP1, PP2CA, which are homologs of AP2C1 and previously reported in K^+ deficiency related functions (Lee *et al*., 2007; Lan *et al*., 2011) revealed that interaction of AP2C1 with CIPK9 is specific and exclusive (Fig. S1, S2).

KIM domain of AP2C1 is necessary and sufficient for interaction

AP2C1 is a MAPK phosphatase and it interacts with MAPKs through its kinase interacting motif (KIM) at N-terminal and mutation in this motif abolishes the interaction (Schweighofer *et al*., 2007; Umbrasaite *et al*., 2010). To investigate whether KIM domain is responsible for AP2C1 and CIPK9 interaction, yeast two-hybrid assay was performed (Fig. 1C). Growth pattern revealed that yeast co-transformed only with CIPK9 and KIM or CIPK9 and K3 (containing PP2C and KIM) grew well on selection medium, while yeast transformed with other construct lacking KIM could not grow. This observation established that AP2C1- KIM domain is necessary and sufficient for the interaction with CIPK9.

AP2C1 interacts with CIPK9 *in planta*

To ascertain AP2C1 and CIPK9 interaction *in planta*, FRET acceptor bleaching analysis was performed wherein, CFP-AP2C1 and YFP-CIPK9 were co-infiltrated into *N. bentahmaiana* cells. Cells showing CFP/YFP signal were scanned for FRET between two proteins. AP2C1 was found to interact with CIPK9 in cytosolic region. Importantly, KIM domain was also found to interact with CIPK9 whereas, K2 domain, which lacks KIM domain does not interact with CIPK9 (Fig. 2A).

Moreover, FRET efficiency was found to be higher for CFP-AP2C1 X YFP-CIPK9 and CFP-KIM X YFP-CIPK9 whereas, almost negligible for CFP-K2 X YFP-CIPK9 and vector control CFP X YFP (Fig. 2B). This observation verified the interaction of AP2C1 with CIPK9 and requirement of KIM domain for the interaction, *in planta*. Furthermore, to validate the interaction, BiFC and co-localization assays were performed. AP2C1 was fused to C-terminal fragment of yellow fluorescent protein (YFP) and CIPK9 was fused to N-terminal of YFP for BiFC assay. Confocal microscope analysis of transformed *N. benthamiana* cells showed that AP2C1-CIPK9 complex is formed in cytosol as YFP signal was reconstituted in cytosolic region (Fig. 3A).

For co-localization, AP2C1-GFP and RFP-CIPK9 were co-transformed in epidermal cells of *N. benthamiana*. Several cells showed strong fluorescence both in GFP and RFP channels and when their signal was merged, yellowish fluorescence was observed at certain locations in the cytosol (Fig. 3B). The co-localization of two proteins was also confirmed by the scatter plot analysis. Thus, overlapping expression and complex formation of AP2C1 and CIPK9 in cytosol is indicative of their concurrent functional requirement in cytosol.

AP2C1 dephosphorylates the auto-phosphorylated CIPK9 *in vitro*

Based on interaction results we hypothesize that CIPK9 might target and phosphorylate AP2C1 or CIPK9 could be dephosphorylated by AP2C1. To test this hypothesis, *in vitro* enzymatic assay was performed. In the assay, purified GST-CIPK9 and GST-AP2C1 proteins (Fig. S3) were used and when ^{32}P radiolabeled GST-CIPK9 was incubated with GST-AP2C1, the level of phospholabeled CIPK9 was reduced. Importantly, no phosphorylation was detected on AP2C1 (Fig. 4A). Upon gradually increasing the concentration of AP2C1 protein while keeping CIPK9 protein concentration constant, gradual decrease in the phospholabel of CIPK9 was detected (Fig. 4B). To confirm the specificity of dephosphorylation, a mutated GST-AP2C1 protein was created, where important Glycine (G) residue at position 178 was substituted by Aspartate (D) through site directed mutagenesis. This mutation in the PP2C catalytic domain has been known to block the phosphatase activity *in vitro* (Sheen, 1998; Meskiene *et al*., 2003). It was observed that mutated AP2C1 (G178D) does not dephosphorylate the auto-phosphorylated CIPK9 (Fig. 4C). These findings confirmed that CIPK9 does not phosphorylate AP2C1 *in vitro*, but AP2C1 dephosphorylates the auto-phosphorylated CIPK9.

The *ap2c1* mutants are tolerant to low-K^+ conditions

Based on AP2C1 and CIPK9 interaction, and dephosphorylation of CIPK9 by AP2C1, we hypothesized that AP2C1 might regulate CIPK9 function in low-K^+ responses. To test this hypothesis, two T-DNA insertion alleles of AP2C1 (*ap2c1-1* and *ap2c1-2*)were analyzed (Fig. 5A, 5B). Also two mutant alleles of CIPK9 (*cipk9-1* and *cipk9-2*) earlier reported by Pandey *et al*., (2007) were used in this analysis.

Phenotype assays were performed for both mutant alleles of *ap2c1* and *cipk9* along with Columbia-0 WT on low K^+ MS media. Seedling growth assays showed slight difference for growth of *ap2c1-1*, *ap2c1-2* and WT at 0 μM K^+, while both *cipk9-1* and *cipk9-2* showed strong hypersensitivity. On 10 μM K^+ medium, visible differences could be seen in the root growth of *ap2c1-1*, *ap2c1-2* and WT. Both the mutant alleles of AP2C1 showed better root growth at 10, 20 and 50 μM K^+ concentration (Fig. 5C; Fig. S4). At 10 mM K^+ concentration (equivalent to concentration of K^+ in 1/2 MS media), there was no difference in the seedling growth of mutant and WT. At most of these low K^+ concentrations, *cipk9* mutant alleles consistently showed hypersensitivity and as the K^+ concentration reached 100 μM, differences in the root growth of *cipk9* mutants and WT diminished. However, *ap2c1* mutant plants showed better root growth even at 100 μM K^+, supported by quantification of relative root growth (Fig. 5D). In depth analysis of the seedlings revealed that *ap2c1* mutants not only had better root growth but also showed better shoot growth. A magnified view of the seedling at 10, 20 and 50 μM K^+ showed that both the mutant alleles of *ap2c1* have bigger and expanded cotyledons than WT, and far better than both *cipk9* mutant alleles. This observation was further supported by quantification of relative fresh weight (Fig. 5E). These findings confirm that while *cipk9* mutant is sensitive, *ap2c1* knockout mutant is tolerant to low-K^+ conditions.

AP2C1 overexpression renders plants sensitive to low-K^+ conditions

To determine the effect of ectopic expression of AP2C1 on plant growth under low-K^+ conditions, we generated overexpression (OX) transgenic lines OX-14 and OX-18 (Fig. 6A, 6B). Both OX-14 and OX-18 showed phenotype opposite to *ap2c1* mutants under low-K^+ conditions and exhibited sensitivity in root growth (Fig. 6C; Fig. S5). While no significant difference was observed in root growth between OX lines and WT at 10 mM K^+, seedlings of both the OX lines showed lesser root growth than WT at 0 μM K^+ to 100 μM K^+. Quantitative analysis supported growth phenotype and maximum difference in the root growth was recorded at 20 μM K^+, where WT showed ~75% relative root growth (w.r.t. control; 10mM K^+) and both the OX lines showed less than 45% root growth (Fig. 6D). Phenotype was also analysed in terms of overall growth and total biomass thereby,

relative fresh weight was estimated for WT and both OX-14 and OX-18. This analysis showed that both OX-14 and OX-18 seedlings had lesser fresh weight than the WT at micromolar K^+ concentrations, while there was no significant difference in fresh weight at 10 mM K^+ (Fig. 6E).

K^+ homeostasis and related gene expression support tolerance of *ap2c1* mutant

To understand the possible mechanism of AP2C1 mutant's tolerance and functional relationship with CIPK9 under low-K^+ condition, total K^+ content was estimated under low and sufficient K^+ growth conditions. Under K^+ sufficient (10mM K^+) conditions WT, *cipk9-1*, *cipk9-2*, *ap2c1-1* and *ap2c1-2* seedlings retained almost similar amount of K^+ (55 mg/g dry weight). Under K^+ deficient conditions (10µM K^+), while WT retained approximately 32mg/g K^+, both the mutant alleles of *cipk9* had lesser K^+ content (23-26 mg/g). On the other hand both *ap2c1-1* and *ap2c1-2* had higher K^+ content (41-44 mg/g) than WT (Fig. 7A). Various K^+ transporters/channels and enzymes are known to be involved in K^+ uptake, transportation and homeostasis. Therefore, to understand the mechanism underlying variable level of K^+ contents in *cipk9* and *ap2c1* mutants, expression analysis was carried out for some of the K^+ transport and homeostasis related genes including, *AKT1*, *CIPK6*, *HAK5* and *LOX2* (Armengaud *et al*., 2004). Under low-K^+ conditions, no significant change was observed in the expression of *AKT1* and *CIPK6* in WT whereas, *HAK5* and *LOX2* had significantly higher expression level. Importantly, expression of all the genes was lower in both *cipk9-1* and *cipk9-2*, whereas expression of *AKT1* and *CIPK6* in both *ap2c1-1* and *ap2c1-2* was higher than *cipk9* mutants and it was comparable to WT. Notably, expression level of *HAK5* and *LOX2* in *ap2c-1* and *ap2c1-2* was much higher than *cipk9* mutants and almost approached to their expression level in WT (Fig. 7B). These findings suggest possible regulatory role of these and similar K^+ homeostasis related genes in uptake and distribution of K^+ ion in *ap2c1* and *cipk9* mutants.

Discussion

In plants, the Ca^{2+} signal generated by K^+ deficiency is majorly decoded by CBL-CIPK complex and transduced downstream by CIPK mediated phosphorylation of target proteins (Luan *et al*., 2009). Specific CBL-CIPK complexes such as CBL1/9-CIPK23 and CBL4-CIPK6 regulate K^+ uptake and distribution in plants through activation of shaker channels AKT1 and AKT2, respectively (Held *et al*., 2011; Xu *et al*., 2006). Ca^{2+} sensing kinases, CDPKs are also implicated in regulation of K^+ ion channels activity (Simeunovic *et al*., 2016; Singh *et al*., 2017). CPK13 phosphorylates two shaker channel subunits KAT1 and KAT2 in the guard cell to control stomata closure (Ronzier *et al*., 2014). Recently, CPK33, in Ca^{2+} dependent manner stimulated the activity of outward-rectifying voltage-

gated K^+ shaker channel GORK in *Xenopus* oocytes thus, CPK33 promotes Ca^{2+} dependent stomata closure (Corratge-Faillie *et al*., 2017). Interestingly, in addition to K^+ uptake CBL1/CBL9–CIPK23 module has also been involved in stomata regulation under dehydrating conditions (Cheong *et al*., 2007). Therefore, involvement of CDPKs in K^+ uptake and distribution is quite possible as both drought stress and K^+ deficiency are interlinked processes in plants (Weinl and Kudla, 2009).

Like CIPK23, CIPK9 is shown to be involved in regulation of low- K^+ signaling in *Arabidopsis* (Pandey *et al*., 2007). It was established as a positive regulator of low-K^+ signaling because its mutants were hypersensitive to low-K^+ conditions. In contradictory, another study showed that CIPK9 might be a negative regulator because they found that *cipk9* mutant plants are more tolerant to low-K^+ conditions (Liu *et al*., 2013). Dissimilar observations by these studies could be accounted by the differences in their experimental procedures including, modified growth media, growth conditions, phenotypes observed and timing of phenotype documentation. In CBL1/CBL9-CIPK23-AKT1 signaling module, AKT1 channel is phosphorylated by CIPK23, and AIP1 (PP2C) dephosphorylate it, thereby reverse the AKT1 channel K^+ uptake activity (Lee *et al*., 2007). In search of upstream and downstream components of CIPK9 mediated K^+ deficiency signaling, we identified another PP2C designated as AP2C1, which interacts with CIPK9 *in vitro* and *in planta*. Previously, AP2C1 was recognised as a MAPK phosphatase and its KIM motif was found responsible for interaction with MAPK4 and MAPK6 (Schweighofer *et al*., 2007). Interestingly, mapping of different region of AP2C1 showed that KIM domain of AP2C1 is necessary and sufficient for interaction with CIPK9 (Fig. 1C, D). Thus, KIM motif could be a conserved structural feature of AP2C1, which might facilitate its interaction with different kinase classes. More importantly, it might be crucial in conferring functional specificity to AP2C1 by governing interaction with different proteins.

In planta interaction analyses for CIPK9 and AP2C1 were carried out in *N. benthamiana* leaves because higher expression of CIPK9 has been observed in leaves than in roots (Pandey *et al*., 2007; Liu *et al*., 2013). Moreover, AP2C1 has been shown to interact with MAPKs in leaf protoplast (Schweighofer *et al*., 2007). These analyses (FRET, BiFC and co-localization) revealed that AP2C1 ineracts with CIPK9 in cytosol, in close proximity to membrane (Fig.2, 3). It could be assumed that in cytosol, CIPK9 might target and regulate K^+ ion channel/transporter located at the membrane (either plasma membrane or endomembrane). It is postulated that CIPKs in general are cytoplasmic proteins and their final cellular destination is influenced by interaction with other protein partners, mainly CBLs (Waadt *et al.*, 2008; Batistič *et al.*, 2010). Channels can also facilitate translocation of CIPKs to the membrane even in absence of CBLs (e.g. AKT1 with CIPK23 and AKT2 with CIPK6) (Xu *et al.*, 2006; Held *et al.*, 2011). Previously, it is shown that CBL2 and CBL3 mediate the

targeting of CIPK9 to tonoplast membrane (Liu *et al*., 2013; Tang *et al*., 2015). However, the target of CIPK9 at tonoplast is not known but it could be assumed that CIPK9 could phosphorylate and regulate crucial two-pore K^+ (TPK1) channel (located at tonoplast membrane) leading to K^+ efflux from vacuole to cytosol, thereby contributing in maintenance of K^+ homeostasis. Recently, CIPK9 was shown to interact with and phosphorylate a plasma membrane localized Ca^{2+} pump ACA8 in *Arabidopsis* (Costa *et al*., 2017). This interaction and phosphorylation event involving ACA8-CIPK9, led to change in stimulus induced cytosolic Ca^{2+} dynamics. Therefore, this could be hypothesized that other transporters/channels such as cation/Ca^{2+} exchangers (CCX), which are involved in cross membrane transportation of cytosolic Ca^{2+} against its electrochemical gradient could also be targeted by CIPK9 to fine tune the cytosolic Ca^{2+} level and to regulate K^+ uptake. Another mode of regulation of K^+ uptake could be transcriptional control of ion channels/transporters through CIPK9. Gene encoding *AtHAK5* is known to be readily induced under low-K^+ condition (Gierth *et al*., 2005). Recently, transcription factor AtARF2 is shown to regulate the expression of *AtHAK5* (Zhao *et al*., 2016). In normal conditions, AtARF2 binds to AtHAK5 promoter and inhibits its expression, whereas under low-K^+ condition AtARF2 is rapidly phosphorylated and detached from AtHAK5 promoter, thereby *AtHAK5* expression is reinstated. Therefore, CIPK9 might phosphorylate similar transcription factor to enhance the transcription of key K^+ channel such as HAK5 under low- K^+ conditions, provided an interacting partner such as CBL translocate CIPK9 to nucleus. However, CIPK9 or its complex with AP2C1 was not found in nucleus, therefore, the possibility of this mode of regulation is miniscule and requires further experimental investigation.

Several plant PP2Cs have been shown to regulate diverse protein kinase pathways in stress and development related processes (Meskiene *et al*., 2003; Kuhn *et al*., 2006; Schweighofer *et al*., 2007). Importantly, multiple CIPKs were found to interact with PP2Cs, such as ABA insensitive 1 (ABI1) and ABI2 (Ohta *et al*., 2003). However, in such interaction, it is unclear whether CIPK phosphorylates PP2C or PP2C dephosphorylates CIPK *in vivo*. Alternatively, a CIPK-PP2C complex might form a kinase/phosphatase signaling module and modulate phosphorylation status of target proteins (Weinl and Kudla, 2009). Therefore, to decipher the meaning of CIPK9-AP2C1 interaction and possible mode of regulation by these two molecules, *in vitro* enzyme activity assay was performed. The biochemical assay revealed that AP2C1 dephosphorylates auto-phosphorylated CIPK9, while CIPK9 does not phosphorylate AP2C1 (Fig. 4). Thus, de-phosphorylation by AP2C1 could be the regulatory mechanism of CIPK9 function, however, *in vivo* confirmation of this mechanism is still awaited.

To determine the functional relevance of CIPK9 regulation by AP2C1, we adopted a genetic approach. Phenotype analysis on low-K^+ media showed that both the *ap2c1* mutant alleles (*ap2c1-1* and *ap2c1-2*) are tolerant to K^+ deficient conditions. In contrast, *cipk9* mutants (*cipk9-1* and *cipk9-2*) were hypersensitive in germination based root growth and seedling development under K^+ deficient conditions (Fig. 5). On the other hand AP2C1 overexpressing lines showed sensitivity to low-K^+ condition, however the sensitivity was not as strong as *cipk9* mutants (Fig. 6). To decipher the tolerance/susceptibility mechanism of AP2C1 and CIPK9 null mutants and possible functional relationship of AP2C1 with CIPK9, dynamics of total K^+ content were analysed. Higher K^+ content of *ap2c1* mutants seedlings (Fig. 7A) suggested that *ap2c1* mutants were able to uptake higher amount of K^+ from the growth environment in deficient conditions and efficiently transport to different parts whereas, *cipk9* mutants were less efficient in K^+ uptake and transportation. This implies that some K^+ uptake, transport and homeostasis related components, possibly regulated by CIPK9 signaling pathway and hence expressed at higher level in *ap2c1* mutants due to removal of AP2C1 inhibition on CIPK9 activity. In order to test this hypothesis, expression analysis for some of the crucial K^+ uptake and homeostasis related genes, including *AKT1*, *CIPK6*, *HAK5* and *LOX2* was undertaken. Supporting variable level of K^+ content, down-regulation of these genes in *cipk9* mutants while relatively higher expression of most of the genes in *ap2c1* mutants were observed (Fig. 7B). These evidences suggest that *HAK5* and *LOX2* might enable the *ap2c1* mutants to uptake and retain higher K^+ content, which could be utilized in vital cellular processes under K^+ deficient conditions. Importantly, contrasting expression pattern of these genes and lesser K^+ content in *cipk9* mutants suggest functional relationship between AP2C1 and CIPK9 in low-K^+ growth conditions. These K^+ uptake and homeostasis related components could be the real targets of CIPK9-AP2C1 modules, however, further experimental evidences are required to verify this hypothesis. These findings also indicate that unlike CIPK23, CIPK9 may not target crucial K^+ channel AKT1, as expression of AKT1 was not significantly altered in *cipk9* or *ap2c1* mutants. In fact, Pandey *et al*., (2007) attempted the interaction of CIPK9 with AKT1 and some other transporters but could not observe any interaction. Moreover, we performed the interaction analysis of AKT1 with AP2C1 in yeast two-hybrid assay but unlike AIP1, AP2C1 does not interact with AKT1 (data not shown). Therefore, CIPK9-AP2C1 possibly constitute a separate signaling cascade of low-K^+ response in *Arabidopsis*.

In conclusion, this study proves that interaction between AP2C1 and CIPK9, and dephosphorylation of CIPK9 by AP2C1 regulate the signaling and response under K^+ deficiency in *Arabidopsis*. This CIPK9-AP2C1 module could be an alternate signaling pathway to an already

established CIPK23-AKT1-AIP1 module or might function in parallel to improve K^+ uptake and/or homeostasis under low K^+ conditions.

Acknowledgements

We are thankful to Prof. Jörg Kudla (Universität Münster, Germany) for providing the pGPTVII.GFP.Kan, pSPYCE-35S^{GW} and pSPYNE-35S^{GW} vectors; Prof. Michael Goodin (University of Kentucky, USA) for pSITE 4CA vectors; and Dr. Irute Meskiene (Max F. Perutz Laboratories, University of Vienna, Austria) for providing *ap2c1-1* (SALK_065126). Arabidopsis Biological Resource Center, Ohio is acknowledged for providing the *ap2c1-2* T-DNA insertion allele (SALK_104445). We also express our thanks to Dr. Kailash C. Pandey (National Institute for Research in Environmental Health, India) for critical reading and comments on this manuscript. We are thankful to Department of Biotechnology (DBT) and University Grant Commission (UGC; UGC-SAP grant), India for research support (in GKP's lab). AS, AKY, IT acknowledge Council of Scientific and Industrial Research (CSIR), India for financial support through research fellowships.

References

Amtmann A, Armengaud P. 2007. The role of calcium sensor-interacting protein kinases in plant adaptation to potassium-deficiency**,** new answers to old questions. Cell Research **17,** 483-485.

Armengaud P, Breitling R, Amtmann A. 2004. The potassium dependent transcriptome of Arabidopsis reveals a prominent role of jasmonic acid in nutrient signaling. Plant Physiology **136,** 2556–2576.

Batistič O, Waadt R, Steinhorst L, Held K, Kudla J. 2010. CBL mediated targeting of CIPKs facilitates the decoding of calcium signals emanating from distinct cellular stores. The Plant Journal **61**, 211–222.

Behera S, Long Y, Schmitz-Thom I, Wang XP, Zhang C, Li H, Steinhorst L, Manishankar P, Ren XL, Offenborn JN, Wu WH, Kudla J, Wang Y. 2017. Two spatially and temporally distinct Ca^{2+} signals convey *Arabidopsis thaliana* responses to K^+ deficiency. New Phytologist **213(2),** 739-750.

Chakrabarty R, Banerjee R, Chung SM, Farman M, Citovsky V, Hogenhout SA, Tzfira T, Goodin M. 2007. PSITE vectors for stable integration or transient expression of autofluorescent protein fusions in plants**,** probing *Nicotiana benthamiana*-virus interactions. Molecular Plant - Microbe Interactions **20,** 740-750.**Ch'erel I, Michard E, Platet N, Mouline K, Alcon C, Sentenac H, Thibaud JB**. 2002. Physical and functional interaction of the *Arabidopsis* K^+ channel AKT2 and phosphatase AtPP2CA. Plant Cell **14,** 1133-1146.

Cheong YH, Pandey GK, Grant JJ, Batistic O, Li L, Kim BG, Lee SC, Kudla J, Luan S. 2007. Two calcineurin B-like calcium sensors, interacting with protein kinase CIPK23, regulate leaf transpiration and root potassium uptake in Arabidopsis. Plant Journal **52(2)**, 223-39.

Corratgé-Faillie C, Ronzier E, Sanchez F, Prado K, Kim JH, Lanciano S, Leonhardt N, Lacombe B, Xiong TC. 2017. The Arabidopsis guard cell outward potassium channel GORK is regulated by CPK33. FEBS Letters **591(13)**, 1982-1992.

Costa A, Luoni L, Marrano CA, Hashimoto K , Köster P, Giacometti S, Michelis MID, Kudla J, Bonza MC. 2017. Ca^{2+}-dependent phosphoregulation of the plasma membrane Ca^{2+}-ATPase ACA8 modulates stimulus-induced calcium signatures. Journal of Experimental Botany 68, 3215-3230.

Gierth M, Mäser P, Schroeder JI. 2005. The potassium transporter AtHAK5 functions in K^+ deprivation-induced high affinity K^+ uptake and AKT1 K^+ channel contribution to K^+ uptake kinetics in Arabidopsis roots. Plant Physiology **137**, 1105– 1114.

Han M, Wu W, Wu W-H, Wang Y. 2016. Potassium Transporter KUP7 Is Involved in K+ Acquisition and Translocation in Arabidopsis Root under K^+-Limited Conditions. Molecular Plant **9**, 437–446.

Held K, Pascaud F, Eckert C, *et al*. 2011. Calcium-dependent modulation and plasma membrane targeting of the AKT2 potassium channel by the CBL4/CIPK6 calcium sensor/protein kinase complex. Cell Research **21,** 1116-1130.

Kuhn JM, Boisson-Dernier A, Dizon MB, Maktabi MH, Schroeder JI. 2006. The protein phosphatase AtPP2CA negatively regulates abscisic acid signal transduction in Arabidopsis, and effects of abh1 on AtPP2CA mRNA. Plant Physiology **140**, 127–139.

Lan WZ, Lee SC, Che YF, Jiang YQ, Luan S. 2011. Mechanistic analysis of AKT1 regulation by the CBL-CIPK-PP2CA interactions. Molecular Plant **4,** 527-536.

Latz A, Mehlmer N, Zapf S, Mueller TD, Wurzinger B, Pfister B, Csaszar E, Hedrich R, Teige M, Becker D. 2013. Salt stress triggers phosphorylation of the Arabidopsis vacuolar K^+ channel TPK1 by calcium dependent protein kinases (CDPKs). Molecular Plant **6**, 1274–1289.

Lee SC, Lan WZ, Kim BG, Li L, Cheong YH, Pandey GK, Lu G, Buchanan BB, Luan S. 2007.A protein phosphorylation/dephosphorylation network regulates a plant potassium channel. Proceedings of the National Academy of Sciences USA **104,** 15959-15964.

Li L, Kim BG, Cheong YH, Pandey GK, Luan S. 2006. A Ca^{2+} signaling pathway regulates a K^+ channel for low-K^+ response in *Arabidopsis*. Proceedings of the National Academy of Sciences USA **103,** 12625-12630.

Liu LL, Ren HM, Chen LQ, Wang Y, Wu WH. 2013. A protein kinase, calcineurin B-like protein-interacting protein Kinase 9, interacts with calcium sensor calcineurin B-like Protein 3 and regulates potassium homeostasis under low-potassium stress in *Arabidopsis*. Plant Physiology **161,** 266-277.

Luan S. 2009. The CBL-CIPK network in plant calcium signaling. Trends in Plant Sciences **14,** 37-42.

Luan S, Lan W, Lee SC. 2009. Potassium nutrition, sodium toxicity, and calcium signaling**,** connections through the CBL-CIPK network. Current Opinion in Plant Biology **12 (3),** 339-346.

Maathuis FJM .2009. Physiological functions of mineral macronutrients. Current Opinion in Plant Biology **12**, 250–258.

Meskiene I, Baudouin E, Schweighofer A, Liwosz A, Jonak C, Rodriguez PL, Jelinek H, Hirt H . 2003. Stress-induced protein phosphatase 2C is a negative regulator of a mitogen-activated protein kinase. Journal of Biological Chemistry **278,** 18945-18952.

Ohta M, Guo Y, Halfter U, Zhu J. 2003. A novel domain in the protein kinase SOS2 mediates interaction with the protein phosphatase 2C ABI2. Proceedings of the National Academy of Sciences, USA **100**, 11771–11776.

Pandey GK. 2008. Emergence of a novel calcium signaling pathway in plants**,** CBL-CIPK signaling network. Physiology and Molecular Biology of Plants **14,** 51-68.

Pandey GK, Cheong YH, Kim BG, Grant JJ, Li L, Luan S. 2007. CIPK9**,** a calcium sensor-interacting protein kinase required for low-potassium tolerance in *Arabidopsis*. Cell Research **17,** 411-421.

Pandey GK, Kanwar P, Pandey A. 2014. Global Comparative Analysis of CBL-CIPK Gene Families in Plants. Springer Briefs Plant Science ISBN 13**,** 978-3-319-09077-1.

Pandey GK, Kanwar P, Singh A, Steinhorst L, Pandey A, Yadav AK, Tokas I, Sanyal S, Lee SC, Cheong YH, Kudla J, Luan S. 2015. CBL-interacting protein kinase, CIPK21, regulates osmotic and salt stress responses in Arabidopsis. Plant Physiology **169**, 780-792.

Pettigrew WT. 2008. Potassium influences on yield and quality production for maize, wheat, soybean and cotton. Physiologia Plantarum **133**, 670–681.

Pyo YJ, Gierth M, Schroeder JI, Cho MH. 2010. High-affinity K^+ transport in Arabidopsis: AtHAK5 and AKT1 are vital for seedling establishment and postgermination growth under low-potassium conditions. Plant Physiology **153**, 863–875.

Ronzier E, Corratge-Faillie C, Sanchez F, Prado K, Briere C, Leonhardt N, Thibaud JB, Xiong TC. 2014. CPK13, a noncanonical Ca^{2+} -dependent protein kinase, specifically inhibits KAT2 and KAT1 shaker K^+ channels and reduces stomatal opening. Plant Physiology **166**, 314–326.

Rubio F, Nieves-Cordones M, Alemán F, Martínez V. 2008. Relative contribution of AtHAK5 and AtAKT1 to K^+ uptake in the high-affinity range of concentrations. Physiologia Plantarum **134(4)**, 598-608.

Sanyal SK, Kanwar P, Yadav AK, Sharma C, Kumar A, Pandey GK. 2017. Arabidopsis CBL interacting protein kinase 3 interacts with ABR1, an APETALA2 domain transcription factor, to regulate ABA responses. Plant Science **254**, 48-59.

Schroeder JI, Ward JM, Gassmann W.1994. Perspectives on the physiology and structure of inward-rectifying K^+ channels in higher plants: biophysical implications for K^+ uptake. Annual Review of Biophysics and Biomolecular Structure **23**, 441–471.

Schweighofer A, Kazanaviciute V, Scheikl E, Teige M, Doczi R, Hirt H, Schwanninger M, Kant M, Schuurink R, Mauch F, Buchala A, Cardinale F, Meskiene I. 2007. The PP2C-type phosphatase AP2C1, which negatively regulates MPK4 and MPK6, modulates innate immunity, jasmonic acid, and ethylene levels in *Arabidopsis*. The Plant Cell **19,** 2213-2224.

Sheen J. 1998. Mutational analysis of protein phosphatase 2C involved in abscisic acid signal transduction in higher plants. Proceedings of the National Academy of Sciences USA **95,** 975-980.

Shin R. 2014. Strategies for Improving Potassium Use Efficiency in Plants. Molecules and Cells **37(8)**, 575-584.

Simeunovic A, Mair A, Wurzinger B, Teige M. 2016. Know where your clients are: subcellular localization and targets of calcium-dependent protein kinases. Journal of Experimental Botany **67**, 3855–3872.

Singh A, Baranwal V, Shankar A, Kanwar P, Ranjan R, Yadav S, Pandey A, Kapoor S, Pandey GK. 2012. Rice phospholipase A superfamily**,** organization, phylogenetic and expression analysis during abiotic stresses and development. PLoS One **7,** e30947.

Singh A, Jha SK, Bagri J, Pandey GK. 2015. ABA inducible rice protein phosphatase 2C confers ABA insensitivity and abiotic stress tolerance in *Arabidopsis*. PLoS One **10,** e0125168.

Singh A, Kanwar P, Pandey A, Tyagi AK, Sopory SK, Kapoor S, Pandey GK. 2013. Comprehensive Genomic Analysis and Expression Profiling of Phospholipase C gene family during Abiotic Stress and Development in Rice. PLoS ONE **8(4)**, e62494

Singh A, Kanwar P, Yadav AK, Mishra M, Baranwal V, Pandey A, Kapoor S, Tyagi AK, Pandey GK .2014. Genome-wide expressional and functional analysis of calcium transport elements during abiotic stress and development in rice. FEBS Journal **281**, 894-915.

Singh A, Pandey A, Srivastava AK, Tran LSP, Pandey GK. 2016. Plant protein phosphatases 2C**,** from genomic diversity to functional multiplicity and importance in stress management. Critical Reviews in Biotechnology **36 (6),** 1023-1035.

Singh A, **Sagar S, Biswas DK**. 2017. Calcium Dependent Protein Kinase, a Versatile Player in Plant Stress Management and Development. Critical Reviews in Plant Sciences **36(5-6)**, 336-352.

Tang R-J, Zhao F-G, Garcia VJ, Kleist TJ, Yang L, Zhang H-X, Luan S. 2015. Tonoplast CBL–CIPK calcium signaling network regulates magnesium homeostasis in Arabidopsis. Proceedings of the National Academy of Sciences, USA **112**, 3134–3139.

Umbrasaite J, Schweighofer A, Kazanaviciute V, *et al*. 2010. MAPK phosphatase AP2C3 induces ectopic proliferation of epidermal cells leading to stomata development in *Arabidopsis*. PLoS One **5,** e15357.

Waadt R, Schmidt LK, Lohse M, Hashimoto K, Bock R, Kudla J.2008. Multicolor bimolecular fluorescence complementation reveals simultaneous formation of alternative CBL/CIPK complexes *in planta*. The Plant Journal **56**, 505–516.

Walker DJ, Leigh RA, Miller AJ. 1996. Potassium homeostasis in vacuolate plant cells. Proceedings of National Academy of Sciences USA **93**, 10510–10514.

Wang Y, Wu WH. 2013. Potassium transport and signaling in higher plants. Annual Review of Plant Biology **64,** 451-476.

Wang Y, Wu W-H. 2017. Regulation of potassium transport and signaling in plants. Current Opinion in Plant Biology **39**, 123–128.

Weinl S, Kudla J. 2009. The CBL-CIPK Ca^{2+}-decoding signaling network**,** function and perspectives. New Phytologist **184,** 517-528.

Xu J, Li HD, Chen LQ, Wang Y, Liu LL, He L, Wu WH. 2006. A protein kinase, interacting with two calcineurin B-like proteins, regulates K^+ transporter AKT1 in *Arabidopsis*. Cell **125,** 1347-1360.

Zhao S, Zhang M-L, Ma T-L, Wang Y. 2016. Phosphorylation of ARF2 Relieves Its Repression of Transcription of the K^+ Transporter Gene HAK5 in Response to Low Potassium Stress. The Plant Cell **28**, 3005–3019.

Zörb C, Senbayram M, Peiter E. 2014. Potassium in agriculture status and perspectives. Journal of Plant Physiology **171**, 656–669.

Figure Legends

Fig 1: Interaction of AP2C1 with CIPK9 by yeast two-hybrid assay. (A) Dilution series of yeast AH109 strains transformed with AD/BD-CIPK9 and AD/BD-AP2C1 constructs. The combination of plasmids is indicated on the left and decreasing cell densities in the dilution series are illustrated by narrowing triangles. Yeast was grown on SC-LW medium, SC-LWH medium or on SC-LWH medium containing 0.5 and 3.0 mM 3-AT. (B) *In vitro* GST pull-down assay. GST-CIPK9 and His-AP2C1 were expressed in *E. coli* and used for analysis. Western blot showing detection of signal using anti-His antibody and loading control is shown by anti-GST antibody. The presence or absence of each protein in the reaction mixture is shown as + or –, respectively. (C) Scheme for making different AP2C1 deletion fragments for interaction analysis with CIPK9. (D) Dilution series of yeast AH109 strains transformed with AD-CIPK9 and BD-AP2C1 or deletion constructs. The combination of plasmids is indicated on the left and decreasing cell densities in the dilution series are illustrated by narrowing triangles. Different negative controls were used which show no growth on selection media.

Fig 2: *In planta* interaction of CIPK9 and AP2C1 by FRET analysis. (A) Fusion constructs of AP2C1, KIM and K2 fragments with cyan fluorescent protein (CFP) and that of CIPK9 with yellow fluorescent protein (YFP) were co-inoculated in *Nicotiana benthemiana* cells. The cells, which showed expression of both CFP and YFP were targeted for FRET by acceptor bleaching protocol. Representative interactions are shown for different FRET combinations. Arrowhead indicates the region of interest (ROI) selected for FRET analysis and to calculate FRET efficiency in individual cells. Scale bar - 20µm. (B) FRET efficiency was calculated from seven different cells, average of seven readings is plotted in bar diagram. For negative control, FRET efficiency was calculated for cells transformed with CFP and YFP containing vectors only. * represents p-value < 0.05, for experimental combinations w.r.t. control (vector only).

Fig 3: Interaction analysis of AP2C1 and CIPK9 by protein pull down, BiFC and Co-localization. (A) *Nicotiana benthamiana* cells co-infiltrated with YFPc:: AP2C1/CIPK9::YFPn showing reconstitution of YFP signal fluorescence in cytosol, while co-infilteration of YFPc:: AP2C1/YFPn and YFPc /CIPK9::YFPn (negative controls) showed no YFP fluorescence, Scale bar = 20 µm. (B) *N. benthamiana* epidermal cells co-transformed with RFP-CIPK9 and AP2C1-GFP showing merge of two signals in the cytosol as yellow fluorescence. Scatterplot showing maximum yellow dots in common region, confirms co-localization of two proteins. Scale bar = 40 µm.

Fig 4: Dephosphorylation of auto-phosphorylated CIPK9 by AP2C1. (A) Autoradiogram showing detection of signals after adding different combination of GST-CIPK9 and GST- AP2C1. Lane of interest is sliced from same autoradiogram/gel and rearranged in close proximity for easy representation of the data. Each sliced part is clearly demarcated by border lines. (B) To determine the dose dependent activity of AP2C1, concentration of GST-AP2C1 was increased gradually from 0 ng to 250 ng while GST-CIPK9 was kept constant at 500 ng in all the reactions. Autoradiogram showing gradual decrease in auto-phosphorylation signal of CIPK9. (C) Gradual increase in the concentration of GST-AP2C1 (G178D) from 0-250 ng did not affect the phosphorylation level of auto-phosphorylated GST-CIPK9. The presence or absence of each protein in the reaction mixture is shown as + or –, respectively.

Fig 5: Germination based phenotypic analysis of AP2C1 and CIPK9 null mutants on K^+ deficient media. (A) The scheme of the *AP2C1* gene structure. Exons (closed boxes) and introns (lines) are indicated. The position of the T-DNA insertion is indicated by an arrowhead. (B) RT-PCR analysis using AP2C1 gene specific primers confirmed the null mutant alleles of AP2C1 (*ap2c1-1*, *ap2c1-2*). Expression of *ACTIN2* was analysed as endogenous control. (C) Germination and vertical growth of *cipk9-1*, *cipk9-2*, WT (Col-0), *ap2c1-1* and *ap2c1-2* on low K^+ concentrations (0µM, 10µM, 20µM, and 50µM) after 7 days. 10mM K^+ concentration is used as control (similar to 1/2 MS). Magnified view of phenotype captured in stereo zoom microscope is shown. Scale bar = 1mm. (D) Quantitative assessment of AP2C1 and CIPK9 null mutant phenotype on K^+ deficient conditions. Relative root growth of *cipk9-1*, *cipk9-2*, WT (Col-0), *ap2c1-1* and *ap2c1-2* on low K^+ concentrations (0µM, 10µM, 20µM, 50µM, 100µM and 10mM) after 7 days. (E) Fresh weight of 7 days old seedlings grown on different K^+ concentrations. 20 seedlings of each genotype were recorded and average of three observations is plotted on the graph ± SD. * p-value < 0.06, ** p-value < 0.03, *** p-value < 0.01..

Fig 6: Germination based phenotypic analysis of AP2C1 overexpression transgenic on K^+ deficient media. (A) Schematic representation of the construct used for overexpression of AP2C1 in *Arabidopsis*. (B) qPCR analysis of two AP2C1 overexpression lines (OX-14 and OX-18) confirms ~ 25 fold higher expression than WT. Each bar represents mean value of three replicates. Standard error among the samples is indicated by error bars. * represents p-value < 0.05 for OX lines w.r.t. WT. (C) Germination and vertical growth of WT (Col-0) and AP2C1 OX lines, OX-14 and OX-18 on low K^+ concentrations (0µM, 10µM, 20µM) after 7 days. Pictures were captured in stereo zoom microscope. Scale bar = 1mm. (D) Relative root growth of WT and AP2C1 OX lines OX-14 and OX-18 on low K^+ concentrations (0µM, 10µM, 20µM, 50µM, 100µM and 10mM) after 7 days. (E) Fresh weight of 7 days old seedlings grown on different K^+ concentrations. 20 seedlings of each genotype were recorded and average of three observations is plotted on the graph ± SD. * p- value < 0.06, ** p-value < 0.03, *** p-value < 0.01..

Fig 7: K^+ ion content and K^+ deficiency related gene expression in *cipk9* and *ap2c1* mutants. (A) K^+ content was calculated in WT, *ap2c1-1*, *ap2c1-2*, *cipk9-1* and *cipk9-2* under K^+ sufficient (10mM K^+) and K^+ deficient (10µM K^+) conditions by atomic absorption spectrophotometry. Experiment was repeated thrice with three biological replicates for each sample. (* $p < 0.05$; ** $p < 0.005$). (B) Relative expression of *AKT1*, *CIPK6*, *HAK5* and *LOX2* in WT, *ap2c1-1*, *ap2c1-2*, *cipk9-1* and *cipk9-2* plants under K^+ deficiency conditions. Expression was analyzed by qPCR and relative expression was calculated by ΔΔCt method using three replicates of each sample. Error bars indicate standard error among the samples. * represents p-value < 0.05 and ** p –value < 0.03 for various genes in different mutants backgrounds w.r.t. WT, under K^+ deficient condition.

Figure 1

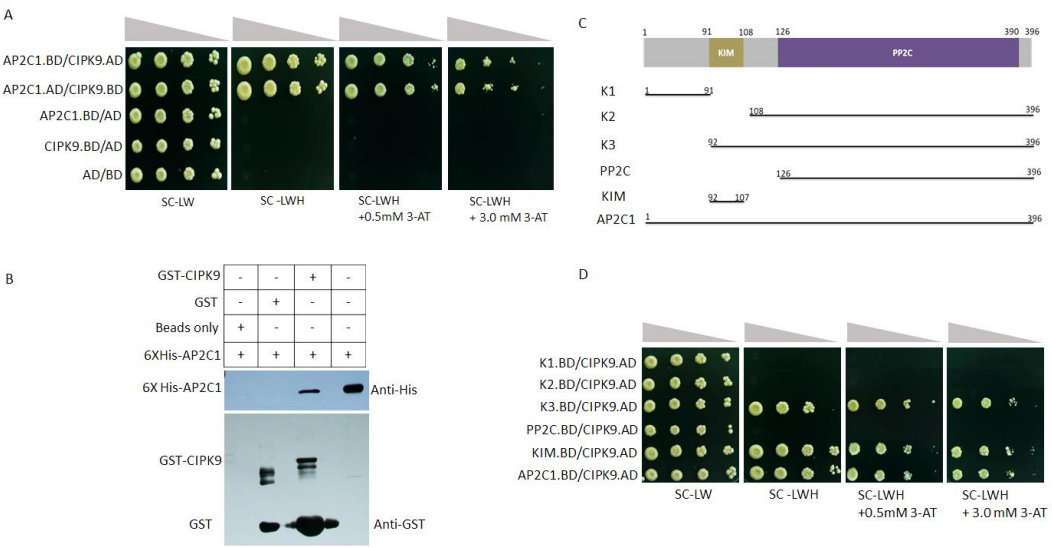

Figure 2

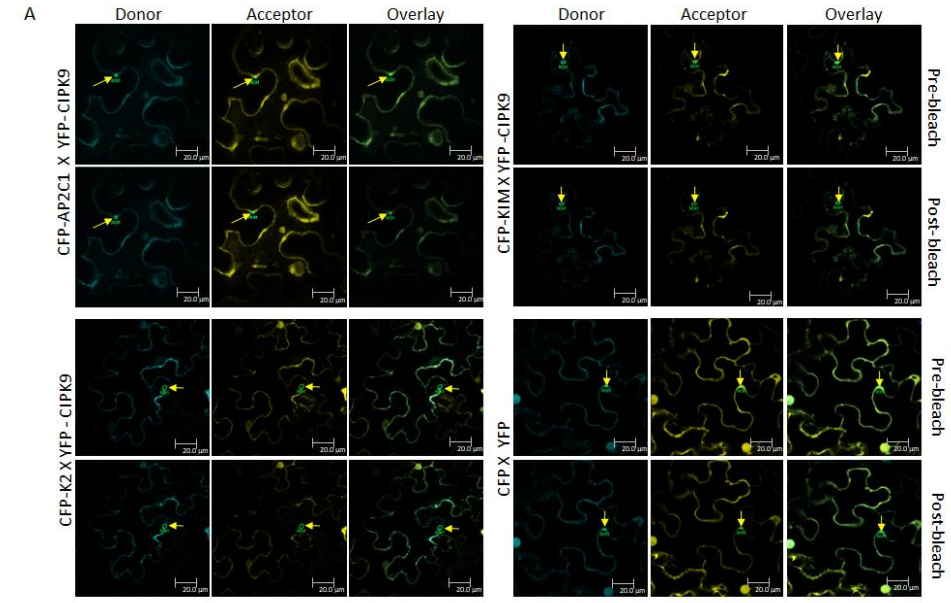

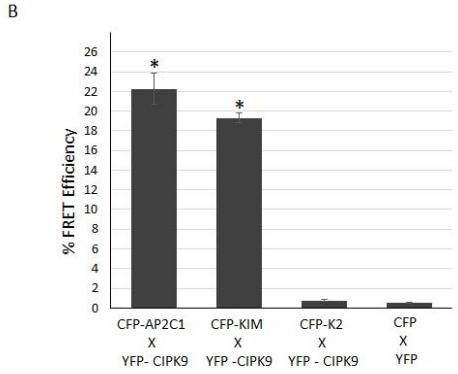

Figure 3

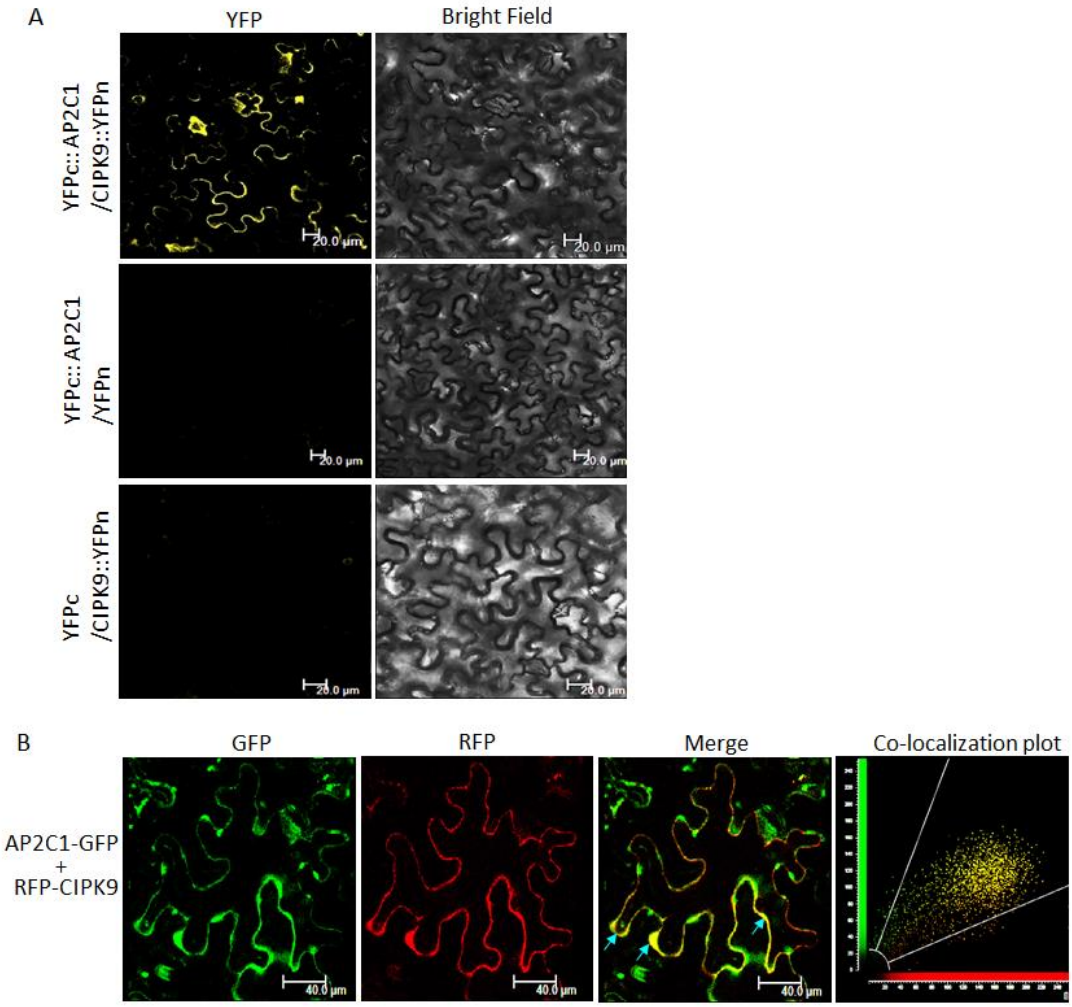

Figure 4

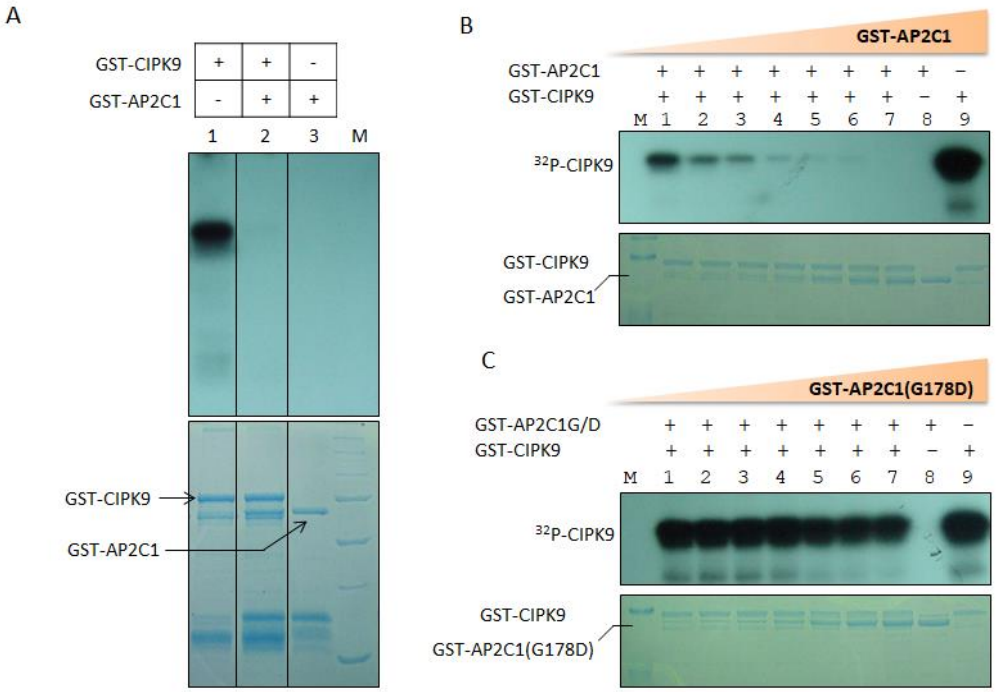

Figure 5

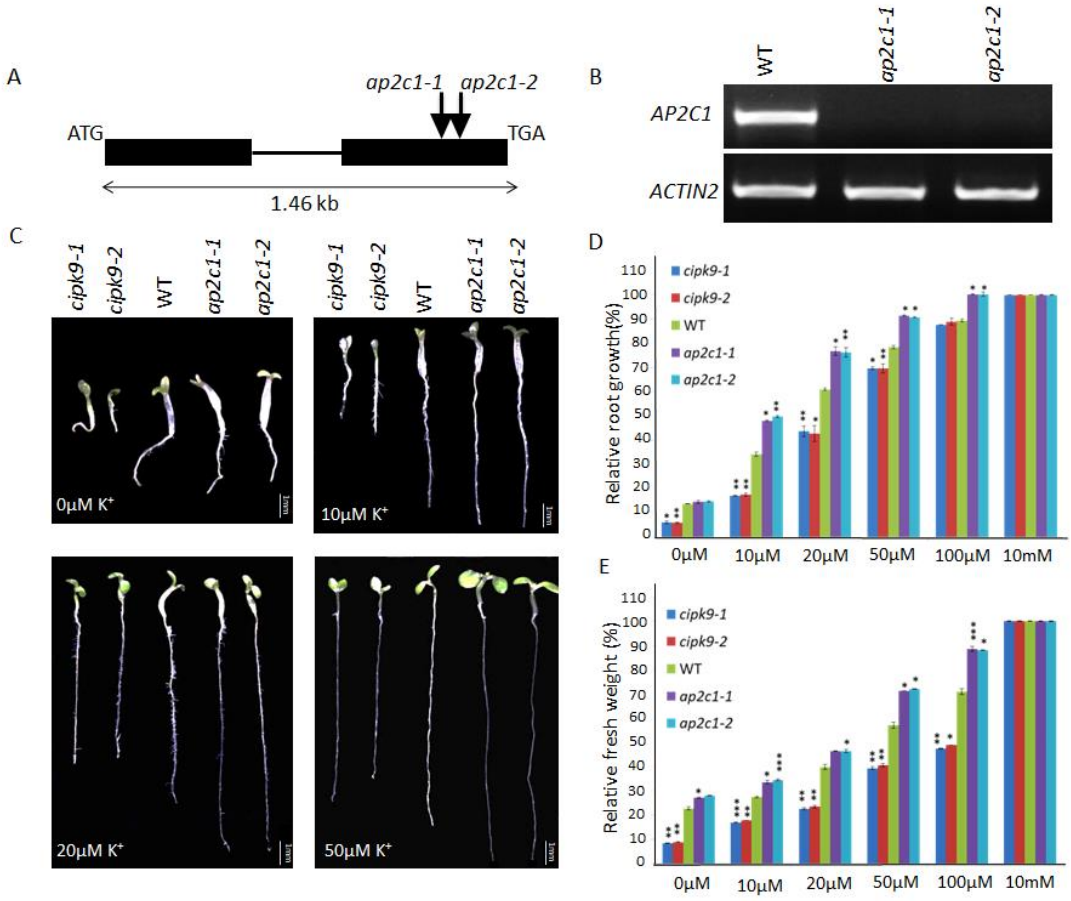

Figure 6

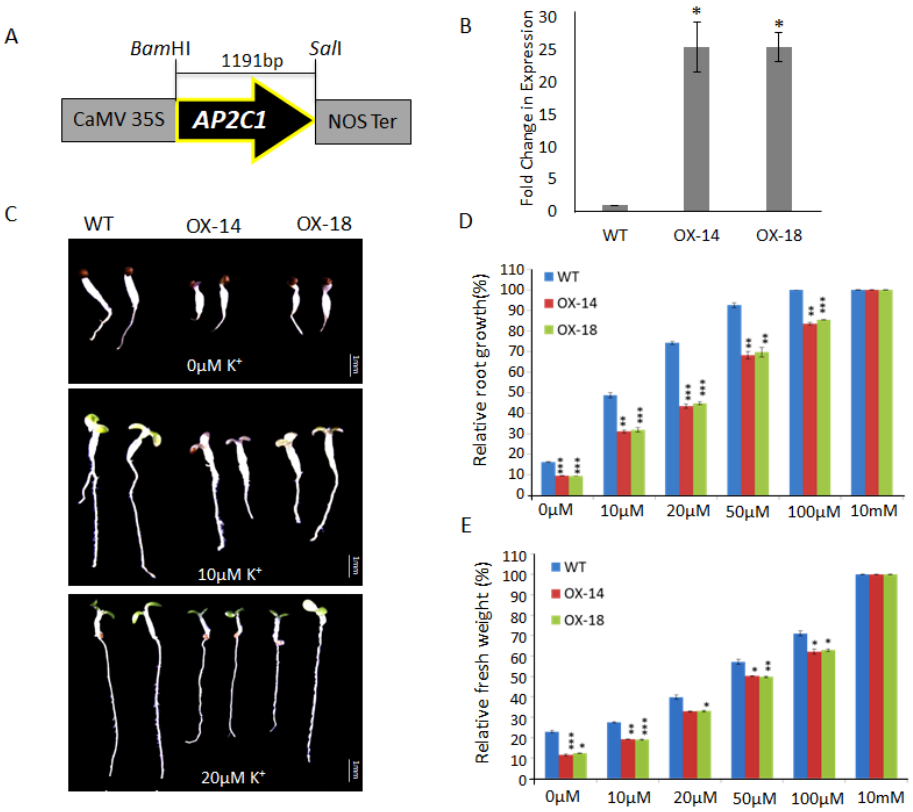

Figure 7